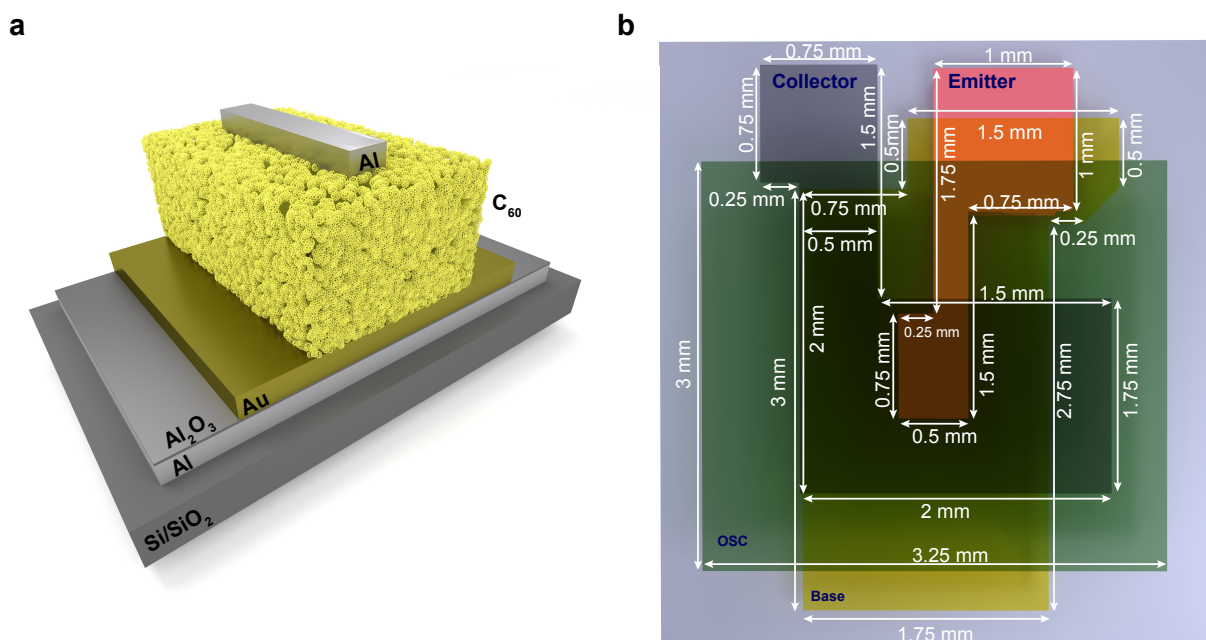


Supporting Information

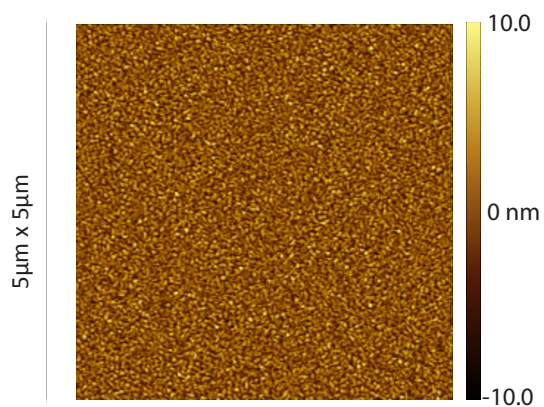
Molecular spectroscopy in a solid-state device

Ainhoa Atxabal, Thorsten Arnold, Subir Parui, Elisabetta Zuccatti, Mirko Cinchetti, Félix Casanova, Frank Ortmann, Luis E. Hueso*

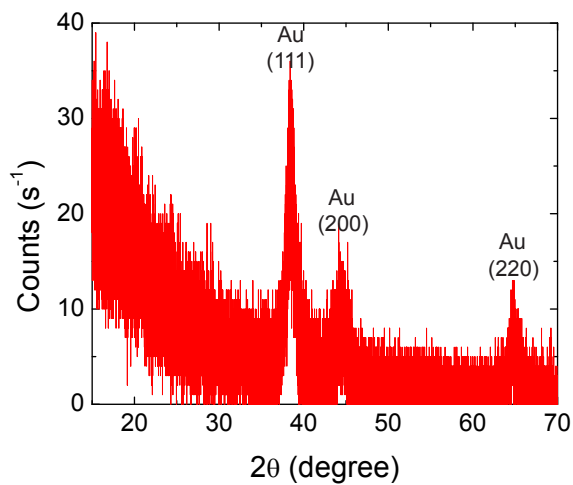
Supplementary Figures



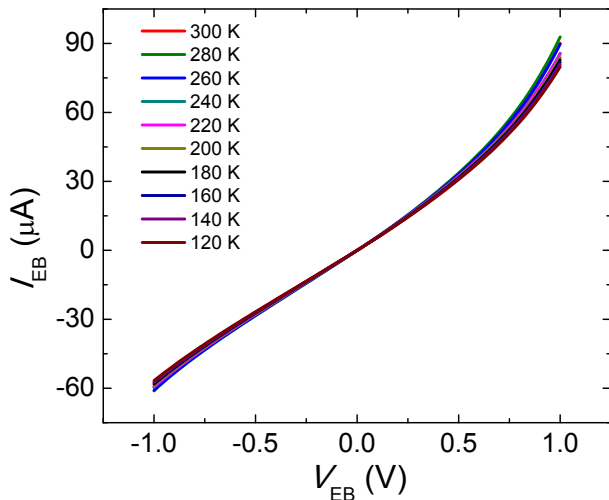
Supplementary Figure 1. Device schematics. a) Schematic cross section of the device. b) Schematics of the top view of the device.



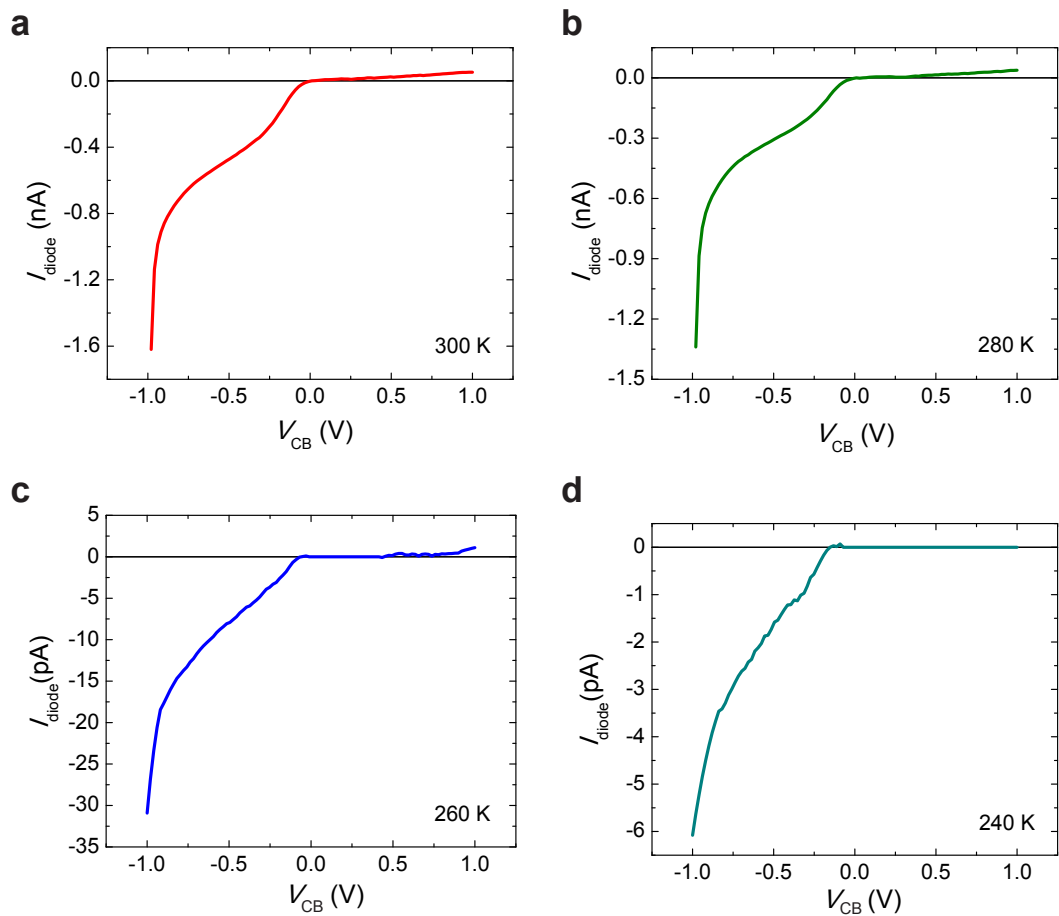
Supplementary Figure 2. Atomic force microscopy (AFM) picture of 200nm of C₆₀. AFM picture of 200nm of C₆₀ thermally evaporated on 10 nm-thick gold thin film with a rate of 0.1 Å s⁻¹. The root mean squared roughness of the film is 1.6 ± 0.1 nm.



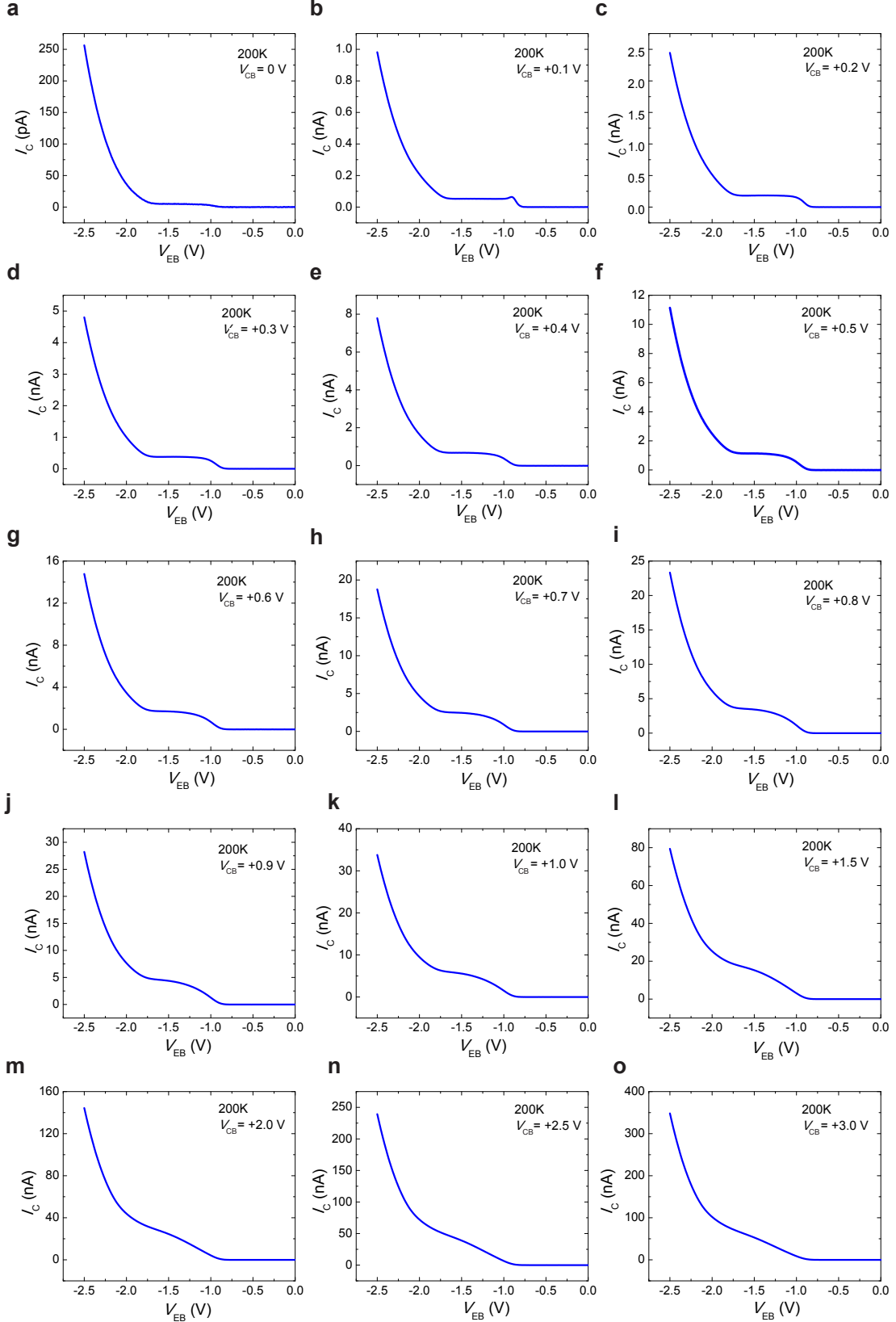
Supplementary Figure 3. X-ray diffraction measurement of 200 nm-thick C_{60} film on 10 nm-thick gold thin film. Three peaks are observed in the diffraction patterned, which corresponds to Au (111), (200) and (220)^[1,2]. No peak has been observed for C_{60} , which ensures its amorphous morphology.



Supplementary Figure 4. Temperature dependence of emitter current, I_E , measured at two terminals in the Al/Al₂O₃/Au junction as function of the applied bias between emitter and base, V_{EB} .

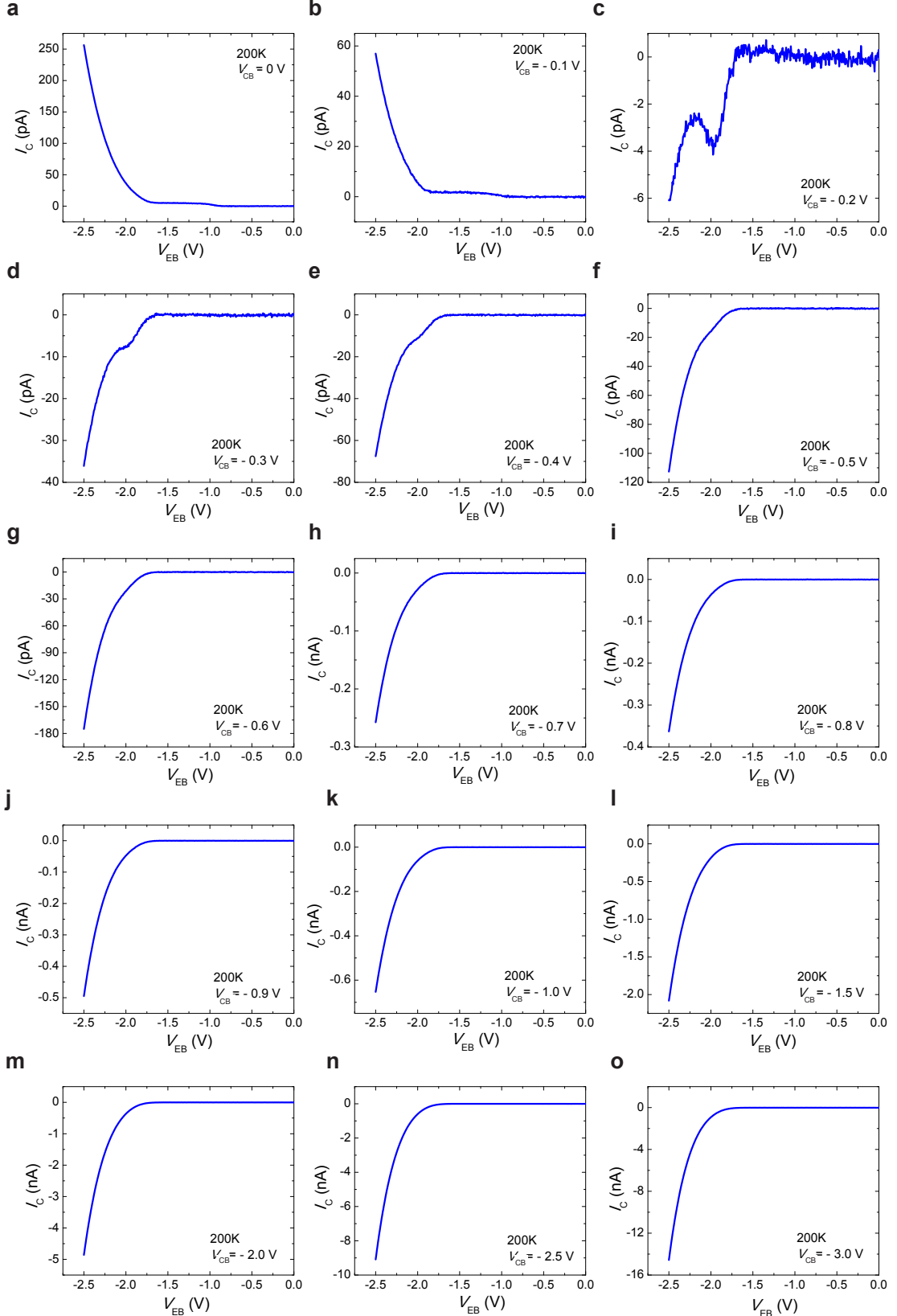


Supplementary Figure 5. Electrical characterization of the Au/C₆₀/Al stack of i-MOS at different temperatures. Current measured at two terminals in the Au/C₆₀/Al stack, I_{diode} , as function of the applied bias between the collector and the base, V_{CB} , at a) 300 K, b) 280 K, c) 260 K and d) 240 K. Negative and positive polarity corresponds to electron injection by the top Al and the base Au, respectively.



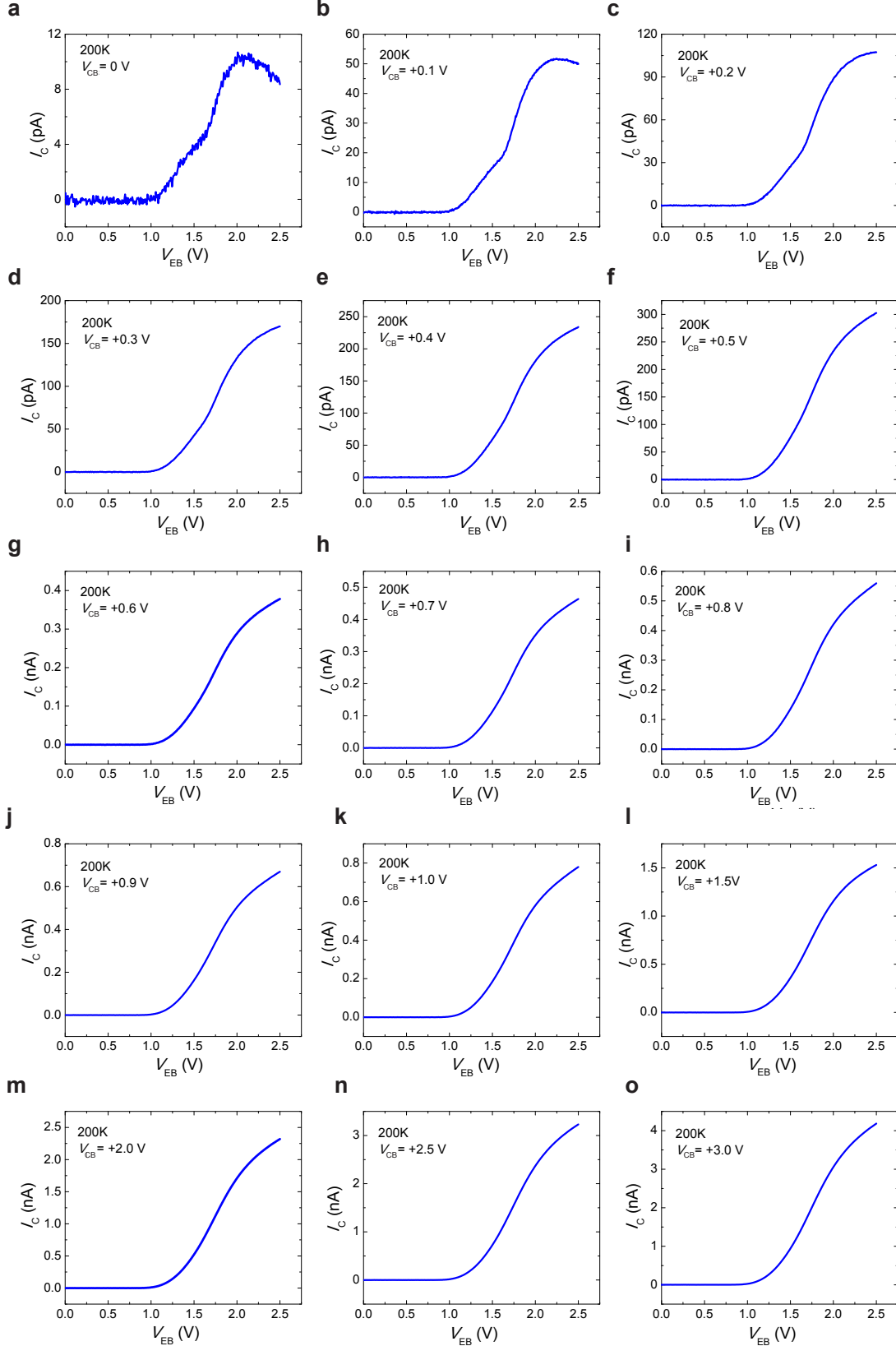
Supplementary Figure 6. Positive collector-base bias, V_{CB} , dependence of collector current I_C for negative emitter-base bias $V_{EB} < 0$ V at 200 K in a Au/C₆₀ based i-MOS. Energetic direct electrons are injected with $V_{CB} \geq 0$ V into the lowest molecular orbital (LUMO) and next higher excited conductive molecular level (LUMO+1) of C₆₀. The lowering of the current observed between LUMO and LUMO+1 when no external V_{CB} bias is applied a), gradually vanishes when

higher positive V_{BC} is applied to the system b-o). The maximum collector current can be modulated three orders of magnitudes (250 pA to 350 nA) by applying a positive collector voltage up to 3 V. Interestingly the onset of LUMO and LUMO+1 remain consistent. Moreover, the current below the first onset is always zero and leakage free.



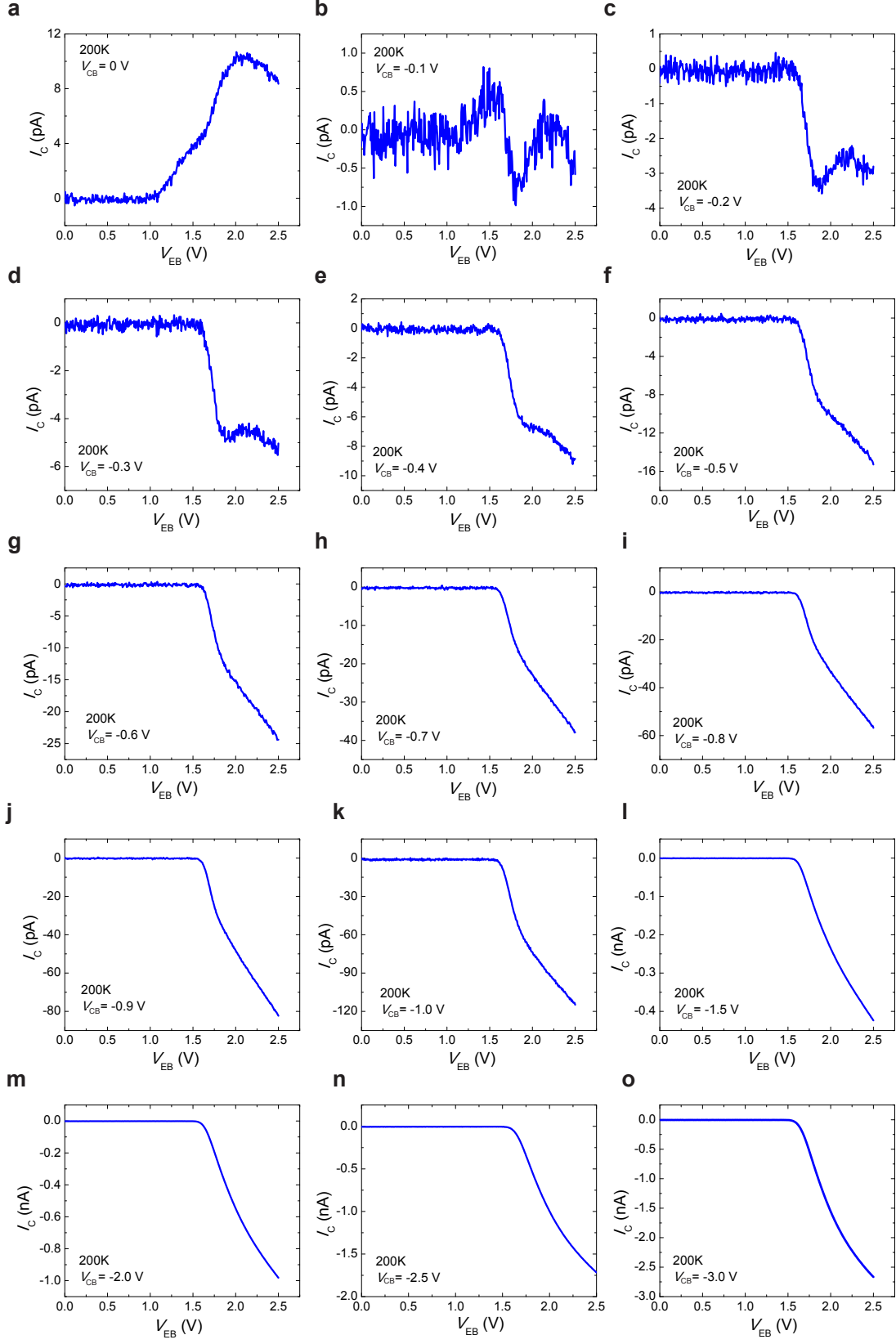
Supplementary Figure 7. Negative collector-base bias, V_{CB} , dependence of collector current I_C for negative emitter-base bias $V_{EB} < 0$ V at 200 K in a Au/C₆₀ based i-MOS device. Energetic primary electrons are injected when $V_{CB} = 0$ V and $V_{CB} = -0.1$ V into the lowest molecular orbital (LUMO) and next higher excited conductive molecular level (LUMO+1) a, b). When $V_{CB} = -0.2$ V, a small direct electron I_C is injected into the LUMO and secondary hole into the HOMO c).

These holes are created by the inelastic scattering of the incident hot electrons in the gold metal base with cold electrons (below the Fermi level) [3]. For lower V_{CB} only secondary holes are injected into HOMO of C₆₀ d-o).

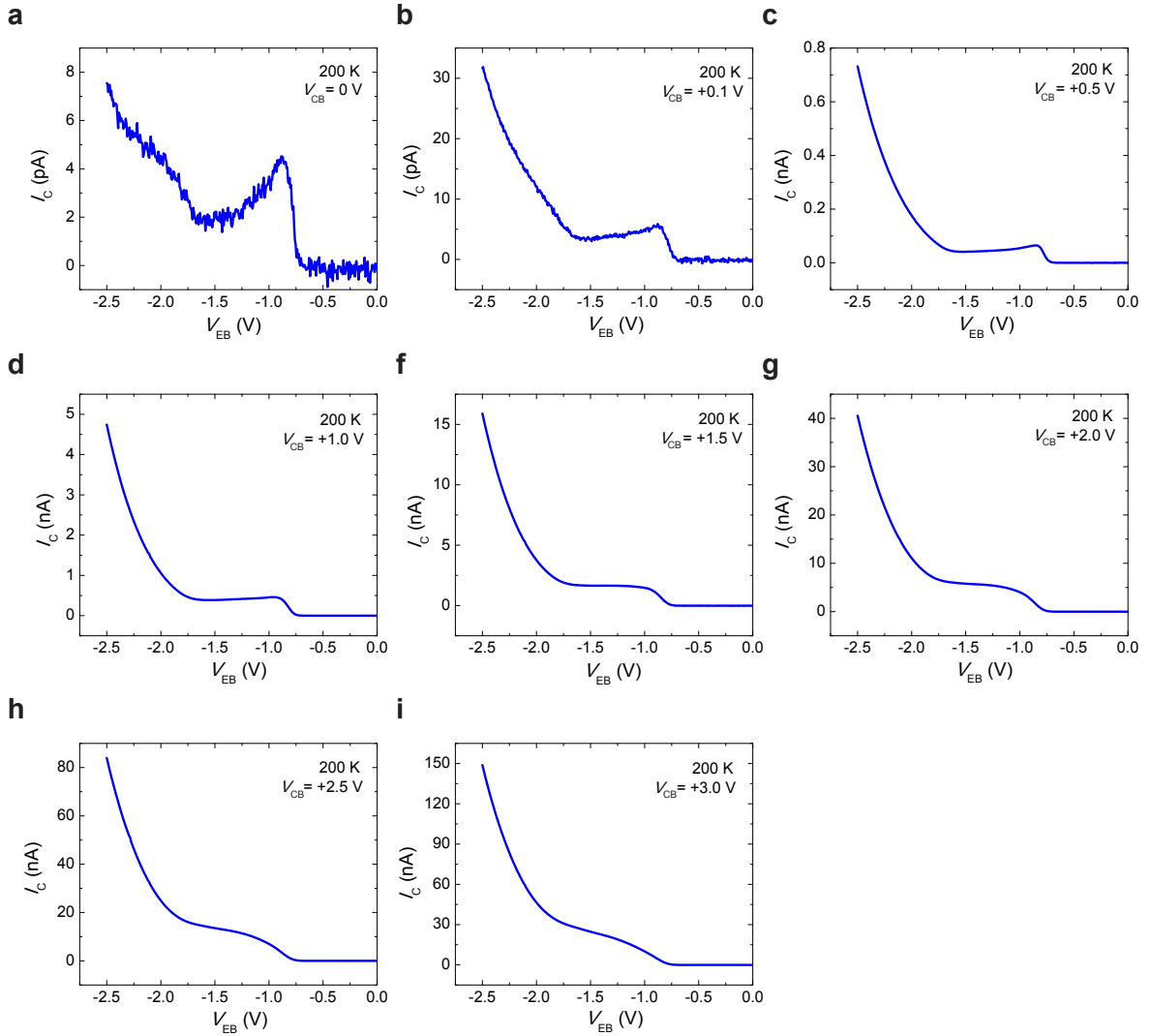


Supplementary Figure 8. Positive collector-base bias, V_{CB} , dependence of collector current I_C for positive emitter-base bias $V_{EB} > 0$ V at 200 K in a Au/C₆₀ based i-MOS device. Energetic secondary electrons are injected when $V_{CB} \geq 0$ V into the lowest molecular orbital (LUMO) a-o). The secondary energetic electron I_C comes from a similar effect to Auger scattering in which

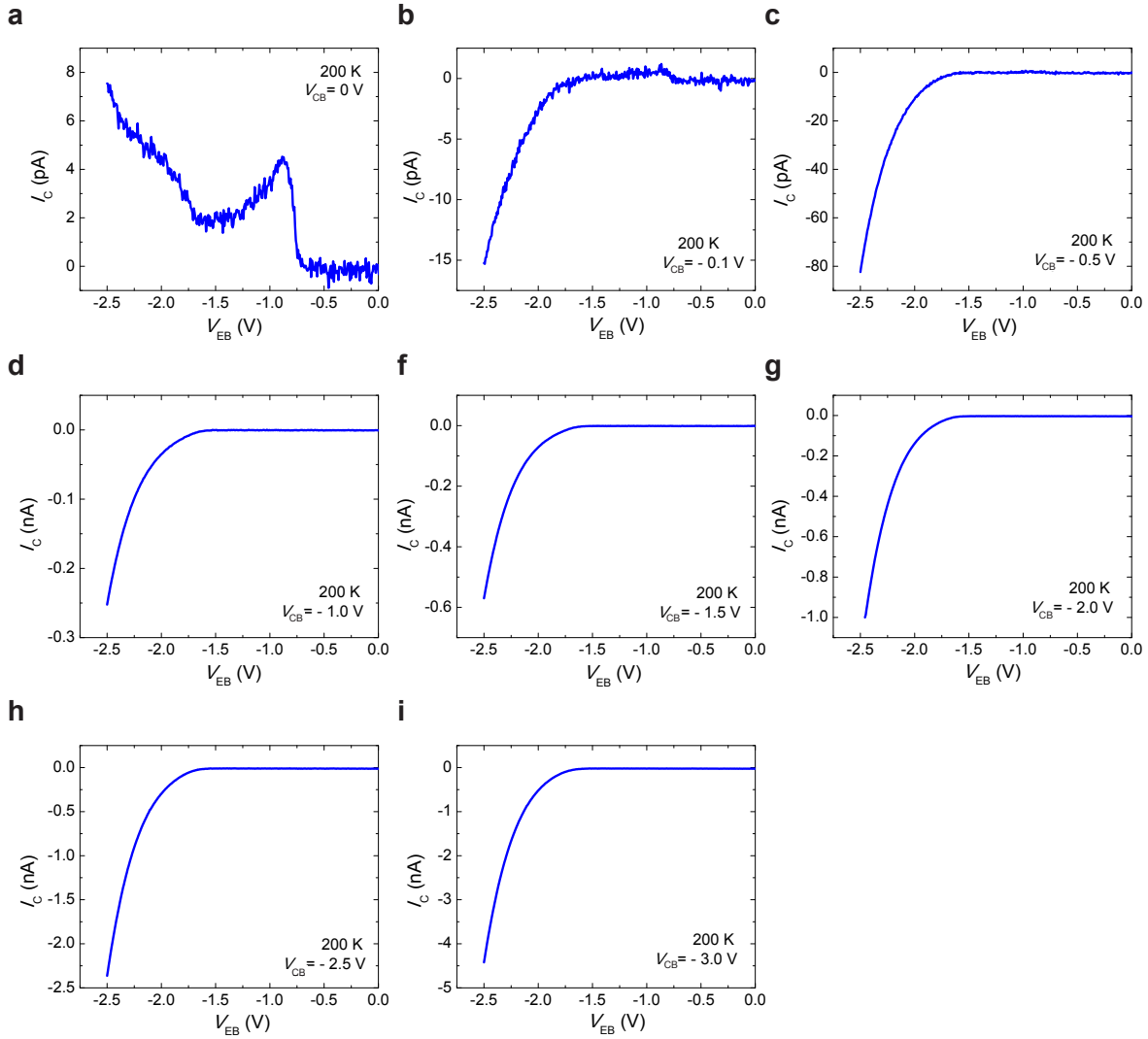
incident energetic holes excite secondary electron-hole pairs in the gold metal base and thus hot electrons are created [4–7]. A contribution from hole I_C might be observed for $V_{CB} = 0.1$ V.



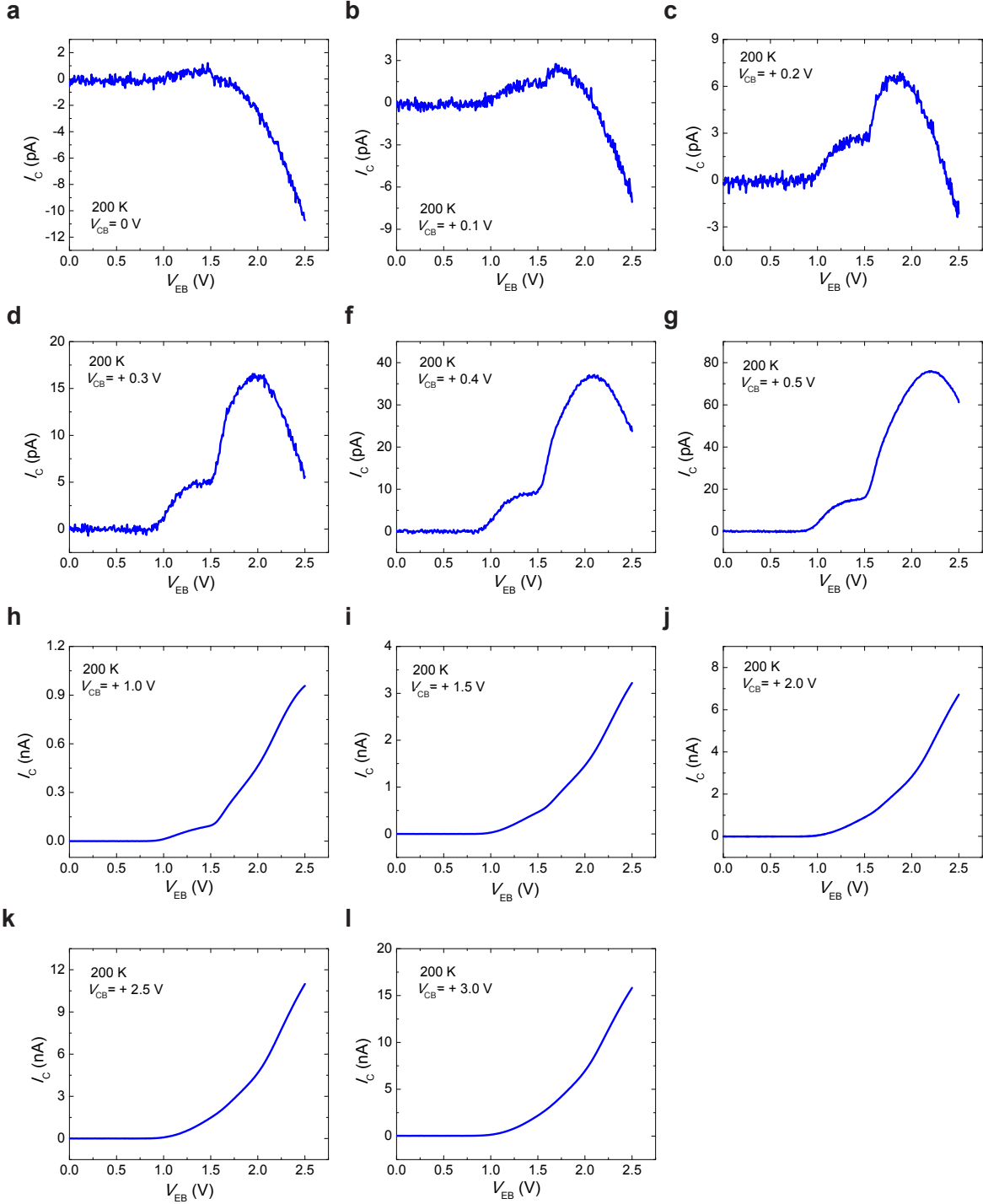
Supplementary Figure 9. Negative collector-base bias, V_{CB} , dependence of collector current I_C for positive emitter-base bias $V_{EB} > 0$ V at 200 K in a Au/C₆₀ based i-MOS. When no V_{CB} is applied secondary electron current coming from similar effect to Auger scattering is observed a). However, when $V_{CB} < 0$ V energetic direct holes are injected leading to the observation of HOMO b-o).



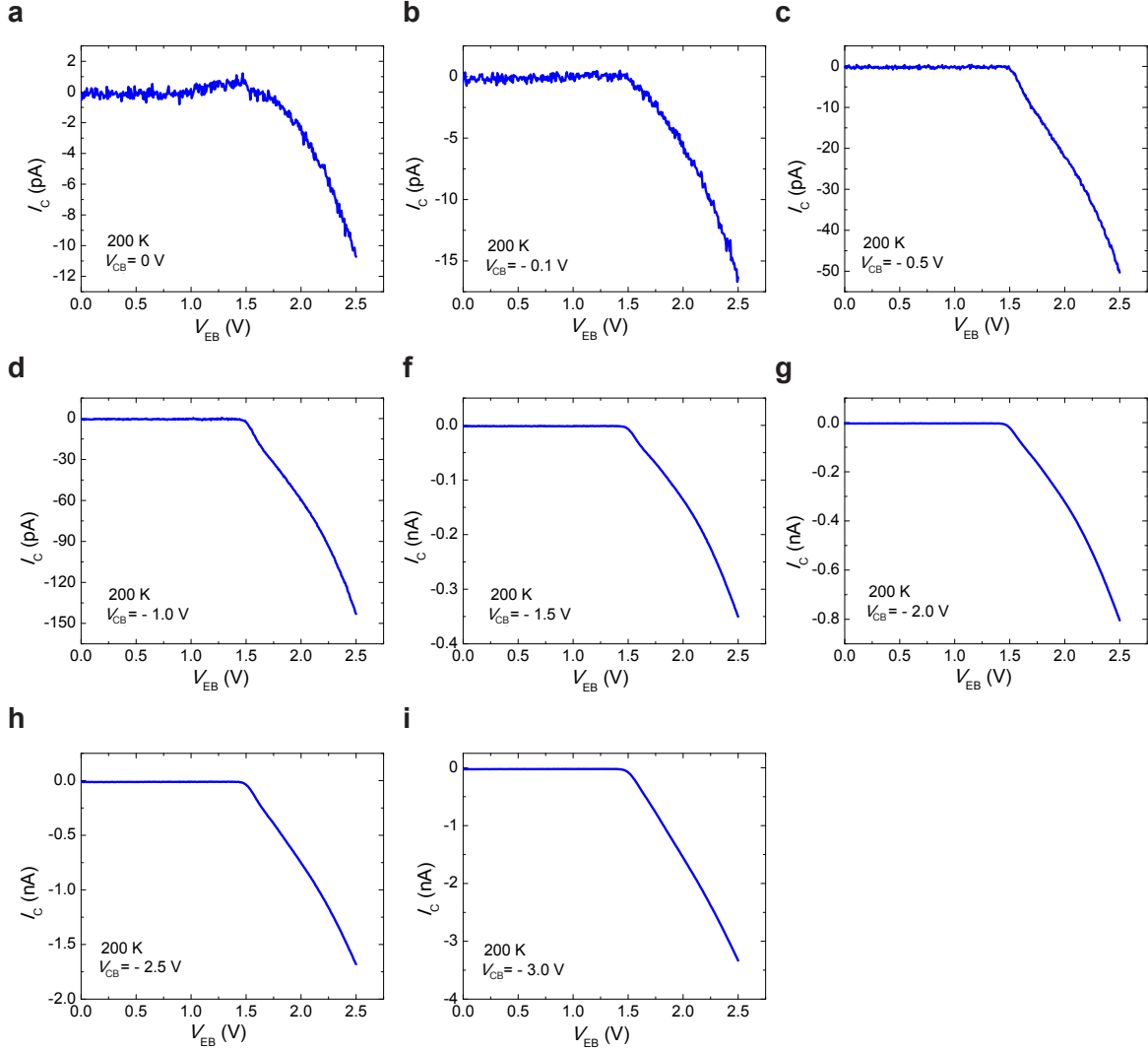
Supplementary Figure 10. Positive collector-base bias, V_{CB} , dependence of collector current I_C for negative emitter-base bias $V_{EB} < 0$ V at 200 K in a Au/C₇₀ based i-MOS. Energetic direct electrons are injected with $V_{CB} \geq 0$ V into the lowest molecular orbital (LUMO) and next higher excited conductive molecular level (LUMO+1) of C₇₀. The lowering of the current observed between LUMO and LUMO+1 when no external V_{CB} bias is applied a), gradually vanishes when higher positive V_{BC} is applied to the system b-i).



Supplementary Figure 11. Negative collector-base bias, V_{CB} , dependence of collector current I_C for negative emitter-base bias $V_{EB} < 0$ V at 200 K in a Au/C₇₀ based i-MOS device. Energetic primary electrons are injected when $V_{CB} = 0$ V into the lowest molecular orbital (LUMO) and next higher excited conductive molecular level (LUMO+1) a). When $V_{CB} = -0.1$ V, a small direct electron I_C is injected into the LUMO and secondary hole into the HOMO b). These holes are created by the inelastic scattering of the incident hot electrons in the gold metal base with cold electrons (below the Fermi level) [3]. For lower V_{CB} only secondary holes are injected into HOMO of C₇₀ c-i).



Supplementary Figure 12. Positive collector-base bias, V_{CB} , dependence of collector current I_C for positive emitter-base bias $V_{EB} > 0$ V at 200 K in a Au/C₇₀ based i-MOS device. When $V_{CB} = 0$ V a) primary hole current is detected together with a small contribution of secondary electron current at LUMO level. Hole current is gradually diminished with $V_{CB} > 0$ V b-g) until only secondary electron current is detected after $V_{CB} = 1.0$ V h-l). The secondary energetic electron I_C comes from a similar effect to Auger scattering in which incident energetic holes excite secondary electron-hole pairs in the gold metal base and thus hot electrons are created [4-7].



Supplementary Figure 13. Negative collector-base bias, V_{CB} , dependence of collector current I_C for positive emitter-base bias $V_{EB} > 0$ V at 200 K in a Au/C₇₀ based i-MOS. When no V_{CB} is applied a small secondary electron current coming from similar effect to Auger scattering is observed together with primary hole current a). However, when $V_{CB} < 0$ V energetic direct holes are injected leading to the observation of HOMO b-i).

Supplementary Tables

Supplementary Table 1. Relative energy of the LUMO, LUMO+1 and HOMO, and transport gap, E_G , of C₆₀ extracted by different Au/C₆₀ based i-MOS devices.

Sample	Device	LUMO (eV)	LUMO+1 (eV)	HOMO (eV)	E_G (eV)
1	1	0.9 ± 0.1	1.8 ± 0.1	1.7 ± 0.1	2.6 ± 0.2
	2	0.9 ± 0.1	1.8 ± 0.1	1.7 ± 0.1	2.6 ± 0.2
	3	0.9 ± 0.1	-	-	-
2	1	0.8 ± 0.1	1.7 ± 0.1	1.6 ± 0.1	2.4 ± 0.2
	2	0.8 ± 0.1	1.7 ± 0.1	1.6 ± 0.1	2.4 ± 0.2
	3	0.8 ± 0.1	1.7 ± 0.1	1.6 ± 0.1	2.4 ± 0.2
3	1	0.9 ± 0.1	1.8 ± 0.1	1.7 ± 0.1	2.6 ± 0.2
	2	0.9 ± 0.1	1.7 ± 0.1	1.7 ± 0.1	2.6 ± 0.2
	3	0.9 ± 0.1	1.8 ± 0.1	1.7 ± 0.1	2.6 ± 0.2
4	1	0.9 ± 0.1	1.7 ± 0.1	-	-
	2	0.9 ± 0.1	1.8 ± 0.1	1.7 ± 0.1	2.6 ± 0.2
	3	0.9 ± 0.1	1.8 ± 0.1	1.7 ± 0.1	2.6 ± 0.2
5	1	0.9 ± 0.1	1.8 ± 0.1	1.7 ± 0.1	2.6 ± 0.2
	2	0.9 ± 0.1	1.8 ± 0.1	1.7 ± 0.1	2.6 ± 0.2
	3	-	-	-	-

Supplementary Table 2. Energy gap of C₆₀ on extracted by different methods. Theory values indicate bulk peak maxima, while experiment commonly refers to the onset of the states. Dependent on the used definition, the difference can be estimated to about 0.4-0.8 eV with larger values from the peak position.

C ₆₀	E _G (eV)	Reference
PES/IPES	2.1	A. J. Maxwell, P. A. Brühwiler, A. Nilsson, N. Mårtensson, P. Rudolfet, <i>Phys. Rev. B</i> , 1994, 49 , 10717.
	2.5	D. Purdie, H. Bernhoff, B. Reihl, <i>Surf. Sci.</i> , 1996, 364 , 279.
STM/STS	2.5	C. Gaul, S. Hutsch, M. Schwarze, K. S. Schellhammer, F. Bussolotti, S. Kera, G. Cuniberti, K. Leo, F. Ortmann, <i>Nat. Mater.</i> , 2018, 17 , 439
	2.7± 0.4	X. Lu, M. Grobis, K. H. Khoo, Steven G. Louie, M. F. Crommie, <i>Phys. Rev. B</i> , 2004, 70 , 115418.
UV-VIS	2.8± 0.1	I. F. Torrente, K. J. Franke, J. I. Pascual, <i>J. Phys. Condens. Matter</i> , 2008, 20 , 184001.
	2.4–2.6	D. Faiman, S. Goren, E. A. Katz, M. Koltun, N. Melnik, A. Shames, S. Shtutina, <i>Thin Solid Films</i> , 1997, 295 , 283.
OTRSR-DFT	2.25	S. Refaelly-Abramson, S. Sharifzadeh, M. Jain, R. Baer, J. B. Neaton, and L. Kronik, <i>Phys. Rev. B</i> , 2013, 88 , 081204.
GW	2.16	S. Refaelly-Abramson, S. Sharifzadeh, M. Jain, R. Baer, J. B. Neaton, and L. Kronik, <i>Phys. Rev. B</i> , 2013, 88 , 081204
GW	3.0	E. L. Shirley, S. G. Louie, <i>Phys. Rev. Lett.</i> , 1993, 71 , 133.
Constr.-DFT	3.26	C. Gaul, S. Hutsch, M. Schwarze, K. S. Schellhammer, F. Bussolotti, S. Kera, G. Cuniberti, K. Leo, F. Ortmann, <i>Nat. Mater.</i> , 2018, 17 , 439.

Supplementary References

- [1] X. Luo, L. Du, Z. Wen, W. Lv, F. Zhao, X. Jiang, Y. Peng, L. Sun, Y. Li, J. Rao, *Nanoscale* **2015**, *7*, 14422.
- [2] Z. Tan, A. Masuhara, S. Ohara, H. Kasai, H. Nakanishi, H. Oikawa, *J. Nanoparticle Res.* **2013**, *15*, 2029.
- [3] L. D. Bell, W. J. Kaiser, *Phys. Rev. Lett.* **1988**, *61*, 2368.
- [4] B. G. Park, E. Haq, T. Banerjee, B. C. Min, J. C. Lodder, R. Jansen, *J. Appl. Phys.* **2006**, *99*, 08S701.
- [5] W. Yi, V. Narayananamurti, H. Lu, M. A. Scarpulla, A. C. Gossard, Y. Huang, J. H. Ryou, R. D. Dupuis, *Appl. Phys. Lett.* **2009**, *95*, 112102.
- [6] W. Yi, V. Narayananamurti, H. Lu, M. A. Scarpulla, A. C. Gossard, *Phys. Rev. B* **2010**, *81*, 235325.
- [7] L. D. Bell, *J. Vac. Sci. Technol. B Microelectron. Nanom. Struct.* **1991**, *9*, 594.